

Accepted Article

Title: Alkyltin Keggin Clusters Templated by Na

Authors: Sumit Saha, Deok-Hie Park, Danielle Hutchison, Lev Zakharov, David Marsh, Sara Goberna-Ferron, Ryan Frederick, John Trey Diiulus, Nizan Kenane, Morgan Olsen, Gregory Herman, Darren Johnson, Doug Keszler, and May Nyman

This manuscript has been accepted after peer review and appears as an Accepted Article online prior to editing, proofing, and formal publication of the final Version of Record (VoR). This work is currently citable by using the Digital Object Identifier (DOI) given below. The VoR will be published online in Early View as soon as possible and may be different to this Accepted Article as a result of editing. Readers should obtain the VoR from the journal website shown below when it is published to ensure accuracy of information. The authors are responsible for the content of this Accepted Article.

To be cited as: *Angew. Chem. Int. Ed.* 10.1002/anie.201701703 *Angew. Chem.* 10.1002/ange.201701703

Link to VoR: http://dx.doi.org/10.1002/anie.201701703 http://dx.doi.org/10.1002/ange.201701703

Alkyltin Keggin Clusters Templated by Na**

Sumit Saha,^[a] Deok-Hie Park,^[a] Danielle C. Hutchison,^[a] Morgan R. Olsen,^[a] Lev N. Zakharov,^[a,c] David Marsh,^[c,d] Sara Goberna-Ferrón,^[a,e] Ryan T. Frederick,^[b] J. Trey Diulus,^[b] Nizan Kenane,^[a] Gregory S. Herman,^[b] Darren W. Johnson,^[c] Douglas A. Keszler,^[a] May Nyman^[a] *

Abstract: Dodecameric (Sn₁₂) and hexameric topologies dominate monoalkyltin-oxo cluster chemistry. Their condensation, triggered by radiation exposure, recently produced unprecedented patterning performance in EUV lithography. Here, we crystallize a new cluster topology from industrial n-BuSnOOH, and additional characterization techniques indicate other clusters are present. Single-crystal X-ray analysis reveals a β -Keggin cluster, which is known but less common than other Keggin isomers in polyoxometalate and The polyoxocation chemistry. structure $[NaO_4(BuSn)_{12}(OH)_3(O)_9(OCH_3)_{12}(Sn(H_2O)_2)],$ (β-NaSn₁₃). NMR, and ESI MS differentiate β -NaSn₁₃, Sn₁₂, and other clusters present in crude 'n-BuSnOOH' and highlight the role of Na as a template for alkyltin Keggin clusters. Unlike other alkyltin clusters that are cationic, $\beta\textsc{-NaSn}_{13}\xspace$ is neutral. Consequently, it stands as a unique model system - absent of counterions - to study the transformation of clusters to films and nanopatterns.

Small oxo-hydroxo metal clusters are transforming the practice of nanolithography.[1] They now offer faster writing speeds, higher resolutions, and better etch resistance than chemically-amplified polymer resists, which have dominated semiconductor manufacturing for decades.^[2,3] First-generation systems, based on Hf sulfate and Nb phosphate clusters in water, exhibited thermally-induced background condensation, which slowed writing speeds and compromised the shelf life of deposition solutions.[4-8] Second-generation systems, based on organo-tin clusters, have suppressed background condensation, allowed radiation-induced condensation to dominate, and increased writing speeds.[1] Yet, only a few organotin clusters are known, and only a subset of them are relevant to highand high-resolution nanolithography. commonly crystallize with charge-balancing counterions, which complicates both the elucidation and understanding of the elementary steps in the lithographic process. Hence, discovery of new charge-neutral organotin

clusters would aid both scientific and technological progress in support of patterning at the extreme end of the nanoscale.

Research on monoalkyltin clusters has produced the well-known dodecameric 'football' $[(RSn)_{12}(O_{14}(OH)_8]^{2+}(Sn_{12})$ and the hexameric 'drum' $[R'Sn(O)O_2CR]_6$ (R=alkyl). $^{[9-13]}$ The less-studied dodecamer $[(2,4,5-iPr_3C_6H_2Sn)_8O_{14}(OH)_8\{Sn(OH)_4\}]$, $^{[14]}$ contains a unique mixture of organic R-Sn and inorganic HO-Sn moieties, the latter resulting from partial dearylation during hydrolysis. Sanchez and co-workers $^{[10b,c]}$ have described the preparation and isolation of Sn_{12} from commercial n-BuSnOOH by refluxing in toluene. Solid-state ^{119}Sn NMR $^{[15]}$ shows 80% of the Sn in n-BuSnOOH occupies six-coordinate environments. Since Sn_{12} contains only 50% six-coordinate Sn, one or more additional species must exist in n-BuSnOOH.

Here, we identify the charge-neutral β -Keggin structure $[NaO_4(BuSn)_{12}(OH)_3(O)_9(OCH_3)_{12}(Sn(H_2O)_2)]$ (β -NaSn₁₃) by methanol dissolution of n-BuSnOOH and crystal growth. The β -isomer is only the second alkyltin Keggin cluster to be synthesized, the first being the γ -isomer. [16] We also find the Na impurity in the commercial material templates the Keggin topology, similar to the structure-directing function of SiO₄⁴⁻ and PO₄³⁻ in polyoxometalates (POMs), and Al/Ga³⁺ in polyoxocations.

A footnote^[17] and supplementary information summarize crystallographic and structural data for $\beta\text{-NaSn}_{13}$ (**fig. 1**). The $\beta\text{-Keggin}$ structure contains four trimers, each built from three edge-shared BuSnO $_5$ octahedra, and the trimers are linked together by corner-sharing. A Na atom occupies the center, and an additional SnO $_6$ cap, orange in Figure 1, bridges two of the trimers shown in gray.

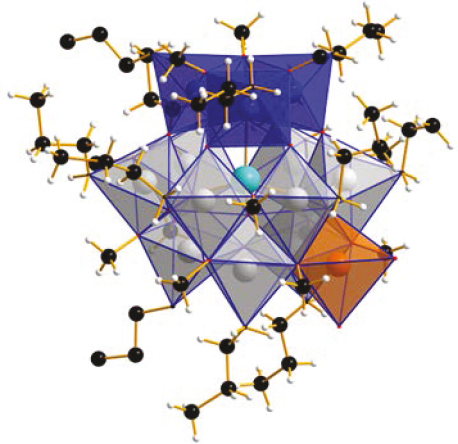


Figure 1. View of β-NaSn₁₃. Gray and blue polyhedra depict the twelve distorted octahedra of the Keggin cluster. The orange polyhedron depicts the capping Sn($H_2O)_2$. The torquoise sphere represents the central Na atom.

The β structure is one of five known Keggin isomers – α , β , γ , δ , and ϵ . All contain four edge-sharing trimers of octahedra that encapsulate a central tetrahedron. The isomers differ by the nature of trimer linking, with α and β linked by corners only, ϵ linked by edges, while γ and δ are linked by a mixture of corner and edge-sharing. The α isomer, ideally point group T_d , transforms to the β isomer, ideally $C_{3\nu}$, by a 60°

[*] contact author information: E-mail: may.nyman@oregonstate.edu
Homepage: http://nyman.chem.oregonstate.edu/
http://sustainablematerialschemistry.org/

[**] This manuscript is dedicated to Roald Hoffman on the occasion of his 80^{th} birthday

Dr. S. Saha, D.-H. Park, D. Hutchison, Dr. S. Goberna-Ferrón, M. Olsen, R.T. Frederick, N. Kenane Prof. G.S. Herman, Prof. D. A. Keszler, Prof. M.

Center for Sustainable Materials Chemistry (CSMC) &

- [a] Department of Chemistry,
- [b] Department of Chemical, Biological & Environmental Engineering Oregon State University; Corvallis, OR 97331 (USA)
- [c] L. N. Zakharov, Dr. D. Marsh, Prof. D. W. Johnson Department of Chemistry and Biochemistry, University of Oregon Eugene, OR 97403 (USA)
- [d] Current address for D.M.: Dept. of Chemistry, Alfred University, Alfred, NY 14802 (USA)
- [e] Current address for S.G.F.: ESRF-The European Synchrotron, 380000 Grenoble (FR)

Supporting information:

rotation of one trimer along the nominal C_3 axis (defined by the blue octahedra in Figure 1). Among polyoxometalate structures, the α isomer occurs more often than β . Weinstock and coworkers have shown heteropolytungstates interconvert between the two structures, which indicates their stabilities can be similar. An organotin-substituted tungstate POMs may adopt the α or β form. Meanwhile, the Al $_{13}$ polycations favor the ϵ -isomer, and there has not been a chemical system identified in which the lower symmetry β and γ Keggin isomers are favored. Therefore the alkyltin Keggin clusters represent a unique opportunity to expand our understanding of the ubiquitous Keggin topology, and is a focus of future research.

The average Na-O bond distance of the central NaO₄ group is 2.32(4) Å. The average Sn-O distance of the corresponding Na-O-Sn linkages is 2.10(2) Å, wherein each O atom is bound by a Na atom and three Sn atoms in μ_4 coordination. The average Sn-O distance of the Sn-OCH₃ linkages is 2.16 (3) Å, where each methoxide bridges two Sn atoms in its μ_3 coordination. The average Sn-O distance for the remaining μ_2 -O ligands is 2.06 (3) Å. These O ligands exist in oxo and hydroxo forms.

A single *n*-butyl group terminates each of the twelve Sn sites in the condensed trimers. The *n*-butyl ligand is absent from the coordination environment of the 13th capping Sn atom. All Sn-O distances (and corresponding bond valence sum. BVS) indicate tetravalent Sn. The cap links to the cluster via two bridging methoxo ligands (Sn-O = 2.2652(1) Å), two bridging oxo ligands (Sn-O = 2.1 (3) Å) and is terminated by two water (H_2O) ligands (Sn-O = 2.3 (3) Å). Metals cations similarly cap polycationic Cr/Al(III) and Fe(III) Keggin ions[21-23] polyanionic Nb(V) Keggin ions[24], and computations have confirmed the roles of metal caps to stabilize Cr and Al polycations.^[21] Because the recrystallization process to obtain β-NaSn₁₃ was very mild (room temperature in methanol), we suspect it was present already in crude n-BuSnOOH. The inorganic tin cap likely originated from a hydrolyzed SnCl₄ impurity. The crystal structure indicates the cluster is charge neutral, because there is no space for counterions in the lattice.

Electrospray ionization mass spectroscopy (ESI MS, **fig. 2**, **fig. SI2-8**, **Table SI2**) provided the first evidence that β -NaSn₁₃ may co-crystallize along with other Keggin topologies from n-BuSnOOH. We identified both +1 and -1 charged species, both capped and uncapped clusters, where uncapped (NaSn₁₂)¹ is the most abundant. The cap may also be removed by the ionization process. These monovalent ions either exist in the recrystallized n-BuSnOOH, or form by protonation of a μ_2 -O or deprotonation of a μ_2 -OH on the parent cluster during the

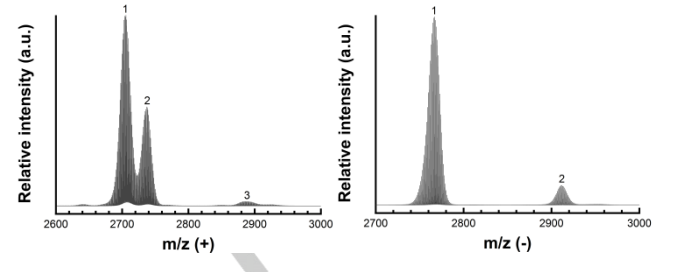


Figure 2. ESI-MS characterization of β-NaSn₁₃ dissolved in methanol Left: the positive ionization mode. Peak identification: 1) [NaO₄(BuSn)₁₂O₆(OH)₆(OCH₃)₁₀]¹⁺, 2) [NaO₄(BuSn)₁₂O₅(OH)₇(OCH₃)₁₁]¹⁺, 3) [NaO₄(BuSn)₁₂O₆(OH)₆(OCH₃)₁₂Sn(OH)_{4-x}(OCH₃)_x]¹⁺. Right: the negative ionization mode. Peak identification: 1) [NaO₄(BuSn)₁₂O₆(OH)₆(OCH₃)₁₂Sn(OCH₃)₂]¹⁻ and/or [NaO₄(BuSn)₁₂O₉(OCH₃)₁₂Sn(OCH₃)₂]¹⁻ and/or [NaO₄(BuSn)₁₂O₉(OCH₃)₁₂Sn(OCH₃)₁₂

ionization process. The infrared spectrum (**Figure SI1**) of the solid shows no broad band around 3500 cm⁻¹, which would indicate the presence of free $\rm H_3O^+$ or OH⁻. Rather, a small sharp peak near 3700 cm⁻¹ reveals the presence of μ_2 -OH ligands. [^{25]} BVS (**Table SI1**) help clarify the charge-neutral formulation of β -NaSn₁₃. The oxos that bridge Na and Sn and the two oxos (O6, O9) that bridge the Sn atoms to the Sn(H₂O)₂ cap are unambiguously O²⁻. The remaining O4, O8, O7, and O31 atoms each possess a BVS between 1.3 and 1.4. The distance (2.5-2.6 Å) between the neighboring O-ligands with ambiguous BVS values is sufficiently short for H⁺ to bridge them (**Figure SI9**), and bridging protonation can play a role in the formulation and structure. The X-ray data do not reveal positions of oxo-bound H-atoms.

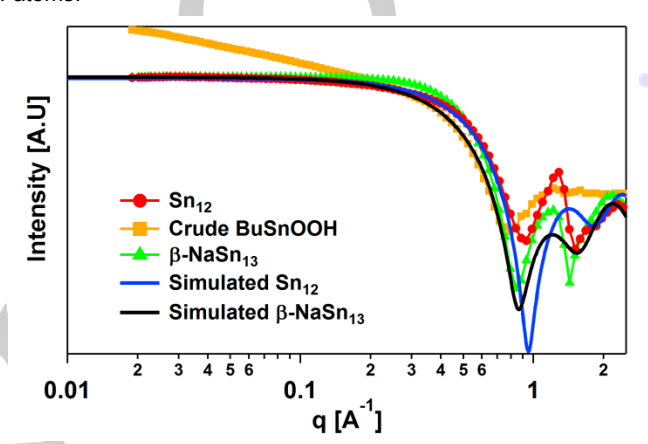


Figure 3. Simulated and experimental SAXS data for THF solutions of n-BuSnOOH, Sn₁₂ and β-NaSn₁₃. See text for discussion. The peak located \sim q=1.5 Å⁻¹ for Sn₁₂ (red) is due to imperfect background subtraction.

Figure 3 shows simulated and experimental small-angle X-ray scattering (SAXS) curves for crude n-BuSnOOH and pure Sn₁₂ and β-NaSn₁₃, all dissolved in THF. The species in each solution are clearly distinguishable by SAXS. The experimental scattering at higher q reveals Sn₁₂ to be a slightly smaller than β-NaSn₁₃, which is also consistent with simulated curves and derived radii of gyration (Table SI3). While the experimental scattering curve for Sn₁₂ matches the simulated curve accurately in the Guinier region, the curve for β-NaSn₁₃ sits between the two simulated curves. This curve has a Coulombic peak that overlaps with the Guinier region, which arises from 'structuring' of the clusters. We attribute this to oleophilic interactions between the butyl chains, which may also contribute to the broadening of the NMR peaks, described below. This differs from Sn₁₂, which shows no such interactions. However, dilution leads to noisier scattering data. Figures SI10 & SI11 show the effect of dilution on the β-NaSn₁₃ scattering data and the modeling of the β-NaSn₁₃ scattering data that includes parameters to describe structuring in solution. By fitting this feature, we get good agreement between the simulated (cluster radius=4.9 Å) and experimental (cluster radius=5.0 Å) scattering curves. Even more convincing, the two observed oscillations of the β-NaSn₁₃ scattering curve (oscillation maxima at q~1.2 & 2.1 Å-1) match the simulated data very well, indicating a solution of Na-centered Keggin ions. The distinct slope in the low q region (q<0.2 Å⁻¹) of *n*-BuSnOOH scattering data instead of the plateau observed in $\beta\textsc{-NaSn}_{13}$ and Sn_{12} indicates the crude material is polydisperse in size, or particles are aggregating. However, a 3phase fit revealed that larger particles or aggregates (radii ~ 20-50 Å) comprise only a few percent of the material, while the

majority is \sim 5 Å radius clusters, consistent with dodecamers. (Figure SI12 & Table SI4).

Two recrystallization steps of crude *n*-BuSnOOH from methanol were required to obtain X-ray-quality crystals. Scanning electron microscope images of these sequentially refined materials are shown in **figure S13**. The infrared spectra (**Figure S1**) of crushed crystals from each crystallization step show the growth of a band at 1039 cm⁻¹ and improved definition of the bands at energies lower than 750 cm⁻¹. The former band corresponds to the C-O stretch of the methoxo ligand, while the latter bands correspond to Sn-O vibrations. The results show – OCH₃ exchanges with –OH during recrystallization and that the crystal-growth process preferentially enriches Na-centered Keggin ions.

We have determined the presence of sodium in both the crude and recrystallized n-BuSnOOH by three independent methods; energy dispersive spectroscopy (EDS), wet chemical analysis and X-ray photoelectron spectroscopy (XPS) (see composite fig. SI14, Table S15). Sodium is detectable in all material forms by all methods. EDS also shows CI is present in the crude material, but not in isolated β-NaSn₁₃. Interestingly, relative Na content determined by both EDS and XPS for twostep recrystallization of β-NaSn₁₃ orders: n-BuSnOOH ~ twicerecrystallized β -NaSn₁₃ > once-recrystallized β -NaSn₁₃. We surmise the manufacturers hydrolyzed n-BuSnCl₃ with NaOH(aq) to produce a crude n-BuSnOOH product. The hydrolysis does not cleanly eliminate NaCl as a byproduct, rather Na templates assembly of clusters such as β -NaSn₁₃. The first recrystallization step shows a decline in Na content (and elimination of CI) via removal of NaCl. The second recrystallization step yields an increase in Na-content by eliminating clusters that are not templated by Na, such as Sn₁₂.

While ESI MS data of n-BuSnOOH (Figures SI15-16) confirm the presence of Na-Sn clusters, i.e., NaSn₁₂ (Keggin without the cap) and NaSn₁₃, the Sn₁₂ signal envelope exhibits the highest intensity. Because MS intensities derive from both species concentration and ionization efficiency, an MS signal alone is not an accurate measurement of relative species abundance. However, 119Sn NMR (Figure SI17) is very informative. Pure β-NaSn₁₃ features broad overlapping peaks between -425 and -475 ppm, consistent with the six-coordinate Sn in the Keggin cluster. Crude n-BuSnOOH also exhibits signals in this region. Sn_{12} has a strong -280 ppm peak consistent with five-coordinate Sn in the 'football' structure. The unidentified -240 ppm peak of n-BuSnOOH is diminished (4% of total integrated area) but not completely eliminated from β-NaSn₁₃. The low symmetry of β -NaSn₁₃ owed to the Sn(H₂O)₂ cap contributes to the complexity of the six-coordinate region of the ¹¹⁹Sn spectrum. Additionally, as noted by ESI MS, there are also uncapped, i.e. NaSn₁₂ clusters present in solution. Surprisingly we cannot observe an ¹¹⁹Sn peak for the inorganic Sn-cap, expected at ~-600 ppm (fig. SI17). We hypothesize that the Sn-cap has labile SnO₆/SnO₅/SnO₄ coordination to the cluster and to methoxy/water ligands, and the signal is broadened into the baseline. Additionally, given the presence of NaSn₁₂ apparent in the ESI MS data, we cannot rule out dilution of β -NaSn₁₃ by cocrystallization of uncapped Keggin clusters. The seven unique BuSn-polyhedra observed in the X-ray structure that yields a complex 119Sn-NMR spectrum likewise confounds interpretation of the ¹H and ¹³C NMR spectra, especially compared to that of Sn_{12} (figs. SI18-19). Both β -NaSn₁₃ and Sn₁₂ have ¹H CH₃ and CH₂ peaks of the butyl chain between 0 and 2 ppm. For Sn₁₂, ¹H-¹H coupling is clearly

observed for two distinct butyl chains, respectively capping the square-pyramidal and octahedral tin. The analogous ¹H peaks for β-NaSn₁₃ are not distinct due to overlap of multiple resonances. While we expect different Sn-polyhedra to yield unique chemicals shifts, the apparent high sensitivity of the butyl ligands to Sn-coordination is surprising. However, we were able to assign these satisfactorily via 2-dimensional experiments including ¹H correlation spectroscopy (COSY) and ¹³C-¹H HSQC (heteronuclear single quantum coherence).(fig. SI20-21) Heating the solution does indeed sharpen these peaks, but it also leads to conversion to Sn12, evidenced by appearance of the 5coordinate 119 Sn peak (fig. SI22). The 13 C butyl peaks of β -NaSn₁₃ are likewise broad and not easily assigned, while those of Sn₁₂ are distinct and assignable. The methoxy ligand is also observed (1H, broad, ~3.5 ppm), overlapping with a sharp peak of free methanol. Heating the solution gives rise to a very broad peak at ~4.2 ppm (fig. Sl23), consistent with hydroxyl ligands that are suggested by BVS and required for charge-balance.

This current study and prior synthesis of Na-centered γ -NaSn₁₂ Keggin isomer^[16] suggests Na $^+$ is an ideal central tetrahedral cation for Keggin ions. In contrast, Dakternieks^[26] synthesized Sn₁₂ in high yield via KOH hydrolysis with no evidence of K $^+$ in the resulting cluster product. We also studied and compared the templating effect of Na by hydrolyzing n-BuSnCl₃ in water with TMAH (tetramethylammonium hydroxide, aq). This reaction yielded a precipitate whose ¹¹⁹Sn NMR spectrum (**Figure Sl15**, **d**) reveals the product to be mainly Sn₁₂; but again, other cluster species are present, indicated by a multitude of peaks.

The first step of alkyltin cluster lithography is deposition of a conformal coating. AFM analysis of β -NaSn₁₃ drop-casted onto graphite shows that is possible to obtain a single monolayer of clusters. (**fig. 4**, figs. **SI24-25**). Low surface coverage from dilute solutions (see SI for experimental detail) yields 20-40 nm wide islands that are 1 nm in height, consistent with the diameter of dodecameric Sn-clusters.

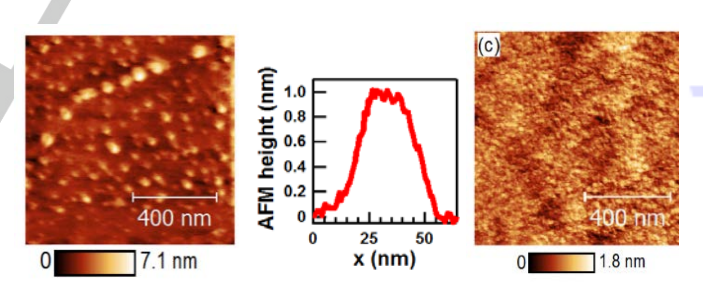


Figure 4. Left: AFM image for 3×10^{-4} M β -NaSn₁₃ drop-cast solution on graphite **middle:** Height profile for cluster isolated on graphite terrace for 1.5×10^{-6} M drop-cast sample. **Right:** Small area scan of spin coated film demonstrating smooth, conformal coating. See **Figures SI24-25** for full image set and height profile location.

In summary, we have structurally characterized a new alkyltin Keggin cluster, namely β -NaSn₁₃, which is templated by Na. Analysis of bulk materials suggests additional unrecognized species form based on hydrolysis conditions; and these are yet to be isolated and structurally characterized. Looking forward, we will exploit several reaction pathways and processes to expand the library of oxo-hydroxo organotin clusters that provide opportunity to study thermally-induced cluster condensation and radiation-induced pattern formation in thin films. Finally, the seemed preference of the lower symmetry Keggin topologies in this emerging family of metal-oxo clusters is unprecedented and

non-intuitive. We will exploit cluster capping, different templating heteroatoms and reaction conditions to further understand Keggin ion isomerization that is recognized, but not well-understood in multiple metal-oxo cluster systems and related materials across the periodic table.

Acknowledgments

This material is based upon the work supported by the National Science Foundation and Center for Sustainable Materials Chemistry under Grant No. CHE-1606982.

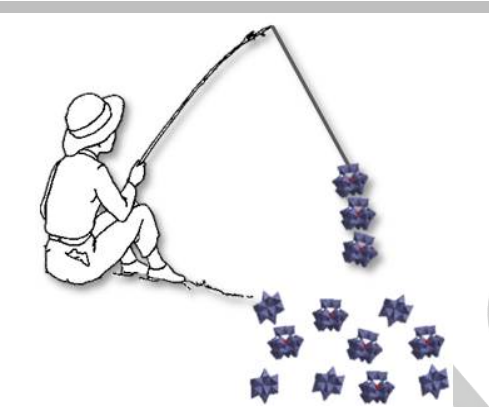
Keywords: alkyltin cluster • small-angle X-ray scattering • Keggin cluster • nanopatterning

- [1] D. Olynick, A. Schwartzberg, D. A. Keszler, Frontiers of Nanoscience: Materials and Processes for Next Generation Lithography, Vol. 11, eds. A. P. Robinson, R. A. Lawson, Elsevier: Amsterdam, 2016, Ch. 10, pp. 349–371.
- [2] D. D. Simone, M. Mao, M. Kocsis, P. De Schepper, F. Lazzarino, G. Vandenberghe, J. Stowers, S. Meyers, B. L. Clark, A. Grenville, V. Luong, F. Yamashita, D. Parnell, Proc. SPIE 9776, Extreme Ultraviolet (EUV) Lithography VII, 2016, 97760B.
- [3] J. Stowers, J. Anderson, B. Cardineau, B. Clark, P. De Schepper, J. Edson, M. Greer, K. Jiang, M. Kocsis, S. Meyers, A. Telecky, A. Grenville, D. De Simone, W. Gillijns, G. Vandenberghe, Proc. SPIE 9779, Advances in Patterning Materials and Processes XXXIII, 2016, 977904.
- [4] R. P. Oleksak, R. E. Ruther, F. Luo, K. C. Fairley, S. R. Decker, W. F. Stickle, D. W. Johnson, E. L. Garfunkel, G. S. Herman, D. A. Keszler, ACS Appl. Mater. Interfaces 2014, 6, 2917–2921.
- [5] J. M. Amador, S. R. Decker, S. E. Lucchini, R. E. Ruther, D. A. Keszler, Proc. of SPIE. 2014, 9051, 90511A, 1–6.
- [6] J.-H. Son, D.-H. Park, D. A. Keszler, W. H. Casey, Chem. Eur. J. 2015, 21, 6727–6731.
- [7] S. Goberna-Ferron, D.-H. Park, J. M. Amador, D. A. Keszler, M. Nyman, Angew. Chem. Int. Ed. 2016, 55, 6221–6224.
- [8] R. E. Ruther, B. M. Baker, J.-H. Son, W. H. Casey, M. Nyman, Inorg. Chem. 2014, 53, 4234–4242.
- [9] H. Puff, H. Reuter, J. Organomet. Chem. 1989, 373, 173-184.
- [10] a) F. Banse, F. Ribot, P. Toledano, J. Maquet, C. Sanchez, Inorg. Chem. 1995, 34, 6371–6379; b) C. Eychenne-Baron, F. Ribot, N. Steunou, C. Sanchez, F. Fayon, M. Biesemans, J. C. Martins, R. Willem, Organometallics 2000, 19, 1940–1949. c)] C. Eychenne-Baron, F. Ribot, C. Sanchez, J. Organomet. Chem. 1998, 567, 137-142.
- [11] a) V. Chandrasekhar, R. O. Day, R. R. Holmes, Inorg. Chem. 1985, 24, 1970–1971; b) R. O. Day, V. Chandrasekhar, K. C. Kumara Swamy, J. M. Holmes, S. D. Burton, R. R. Holmes, Inorg. Chem. 1988, 27, 2887–2893.
- [12] V. Chandrasekhar, S. Nagendran, S. Bansal, A. Wallace Cordes, A. Vij, Organometallics 2002, 21, 3297–3300.
- [13] S. U. Ahmad, J. Beckmann, A. Duthie, Organometallics 2009, 28, 7053–7054.
- [14] G. Prabusankar, B. Jousseaume, T. Toupance, H. Allouchi, Angew. Chem. Int. Ed. 2006, 45, 1255–1258.
- [15] F. Ribot, C. Eychenne-Baron, F. Fayon, D. Massiot, B. Bresson Main Group Metal Chemistry 2002, 25, 115-119.
- [16] H. Reuter, Angew. Chem. 1991, 103, 1487–1489.
- [17] $C_{60}H_{73}NaO_{30}Sn_{13}$, M=2840.14, $0.08 \times 0.06 \times 0.03$ mm, T=173(2) K, Orthorhombic, space group Pnma, a=32.2623(19) Å, b=19.3472(11) Å, c=16.0513(8) Å, $\alpha=\beta=\gamma=90^\circ$, V=10019.0(10) ų, Z=4, $D_c=1.883$ Mg/m³, $\mu(Cu)=25.851$ mm⁻¹, F(000)=5336, $2\theta_{max}=106.6^\circ$, 33878 reflections, 6000 independent reflections [R_{int}=0.0818], R₁=0.1277, wR₂=0.3115 and GQF=1.113 for 6000 reflections (502 parameters) with $I>2\sigma(I)$, $R_1=0.2049$, wR₂=0.3912 and GQF=1.158 for all reflections, max/min residual electron density=+1.780/-2.024 eÅ⁻³. Depository number CCDC-1527536.

- [18] I. A. Weinstock, J. J. Cowan, E. M. G. Barbuzzi, H. Zeng, C. L. Hill, J. Am. Chem. Soc. 1999, 121, 4608–4617.
- [19] F. Xin, M. T. Pope, G. J. Long, U. Russo, Inorg. Chem. 1996, 35, 1207– 1213.
- [20] C. A. Ohlin, J. R. Rustad, and W. H. Casey, Dalton Trans. 2014, 43, 14533-14536.
- [21] W. Wang, L. B. Fullmer, N. A. G. Bandeira, S. Goberna-Ferron, L. N. Zakharov, C. Bo, D. A. Keszler, M. Nyman, Chem 2016, 1, 887–901.
- [22] O. Sadeghi, C. Falaise, P. I. Molina, R. Hufschmid, C. F. Campana, B. C. Noll, N. D. Browning, M. Nyman, Inorg. Chem. 2016, 55, 11078–11088.
- [23] O. Sadeghi, L. N. Zakharov, M. Nyman, Science 2015, 347, 1359–1362.
- [24] Y. Hou, L. N. Zakharov, M. Nyman, J. Am. Chem. Soc. 2013, 135, 16651– 16657.
- [25] T. M. Alam, M. Nyman, B. R. Cherry, J. M. Segall, L. E. Lybarger, J. Am. Chem. Soc. 2004, 126, 5610–5620.
- [26] D. Dakternieks and H. Zhu, E.R.T. Tiekink, R. Colton, J. Organomet. Chem. 1994, 476, 33-40.

COMMUNICATION

Fishing for facts. Solution phase characterization of n-BuSnOOH and structure determination of a butyltin, Na-centered β-Keggin cluster extracted from this crude mixture brings new understanding to this widely used compound in materials science and chemistry. Advances in nanolithography and alkyltin cluster chemistry will ensue.



Sumit Saha, Deok-Hie Park, Danielle Hutchison, Morgan Olsen, Lev N. Zakharov, David Marsh, Sara Goberna-Ferron, Ryan T. Frederick, J. Trey Diulus, Nizan Kenane, Gregory S. Herman, Darren W. Johnson, Douglas A. Keszler, May Nyman*

Page No. – Page No.

Self-assembly of Alkyltin Dodecameric Topologies